Liver CT Image Segmentation with an Optimum Threshold using Measure of Fuzziness

Abder-Rahman Ali[1], Micael Couceiro[2,3], Ahmed M. Anter[4,1], Abul Ella Hassenian[1,5], Mohamed F. Tolba[6] and Vaclav Snasel[7]

[1]Scientific Research Group in Egypt (SRGE), Egypt
[2]Artificial Perception for Intelligent Systems and Robotics (AP4ISR), Institute of Systems and Robotics (ISR), University of Coimbra, Portugal
[3]Ingeniarius, Lda., Rua da Vacaria, n.37, 3050-381, Mealhada, Portugal
[4]Faculty of Computers and Information, Mansoura University, Egypt
[5]Faculty of Computers and Information, Cairo University, Egypt
[6]Faculty of Computers and Information, Ain Shams University, Egypt
[7]Electrical Engineering & Computer Science,VSB-TU Ostrava

Abstract. This paper presents a Fuzzy C-Means based image segmentation approach with an optimum threshold using measure of fuzziness. The optimized version, herein denoted as FCM-**t**, benefits from an optimum threshold, calculated using measure of fuzziness. This allows the revealing of ambiguous pixels, which are eventually assigned to the appropriate clusters by calculating the rounded average cluster values in the ambiguous pixels neighbourhood. The proposed approach showed significantly better results compared to the traditional Fuzzy C-Means, at the cost of some processing power. By benefiting from the optimum threshold approach, one is able to increase the segmentation performance by approximately three times more than with the traditional *FCM*.

Keywords: Segmentation, fuzzy C-means, threshold, clustering

1 Introduction

Image segmentation is the process of subdividing the image into its constituent parts, and is considered one of the most difficult tasks in image processing. It plays a vital role in any application and its success is based on the effective implementation of the segmentation technique [1]. For many applications, segmentation reduces to finding an object in an image. This involves partitioning the image into two classes: objects or background [2]. Recent advances in a wide range of medical imaging technologies have revolutionized how we perceive functional and pathological events in the body and define anatomical structures in which these events take place. Medical images, in their raw form, are represented by arrays of numbers in the computer, with the numbers indicating the values of relevant physical quantities that show contrast between different types of body tissue. Processing and analysis of medical images are useful in transforming raw images into a quantifiable symbolic form for ease of searching

and mining, in extracting meaningful quantitative information to aid diagnosis, and in integrating complementary data from multiple imaging modalities. One fundamental problem in medical image analysis is image segmentation, which identifies the boundaries of objects, such as organs or tumors Having the segmentation result makes it possible for shape analysis, detecting volume change, and making a precise radiation therapy treatment plan. However, despite the intensive research, segmentation remains a challenging problem due to the diverse image content, cluttered objects, occlusion, image noise, non-uniform image texture, *etc* [3].

Spiral computed tomography (CT) has rapidly gained acceptance as the preferred CT technique for routine liver evaluation because it provides image acquisition at peak enhancement of the liver parenchyma during a single breath hold [4]. The liver is a large, meaty organ that sits on the right side of the belly. Weighting about three pounds, the liver is reddish-brown in colour and feels rubbery to the touch [5]. It fulfills multiple and finely tuned functions that are critical for the homeostasis of the human body. Although individual pathways for synthesis and breakdown of carbohydrates, lipids, amino acids, proteins, and nucleic acids can be identified in other mammalian cells, only the liver performs all these biochemical transformations simultaneously, and is able to combine them to accomplish its vital biological task. The liver is also the principal site of biotransformation, activation, or inactivation of drugs and synthetic chemicals. Therefore, this organ displays a unique biologic complexity. When it fails, functional replacement presents one of the most difficult challenges in substitutive medicine [6]. Due to its unreplaceable attributes, much of the research on medical imaging over the past few years has been centered on studying CT images of the liver. As such, researchers across the globe have been working towards providing a diagnostic support of liver diseases, liver volume measurements, and 3D liver volume rendering, without the need of any manual process and visual inspection, which are a mental work and a huge time consuming process. Image segmentation has been one of the many image processing methods employed on that particular task. Nevertheless, still many challenges remain before one can provide a fully autonomous image segmentation method of liver CT images. The physical attributes of the liver previously described, combined with the limitations inherent to CT technology, are translated into low-level contrast and blurry edged images, varying from patient to patient and between different CT processes. Additionally, other organs in the vicinities, like spleen and stomach, share similar gray levels, thus making it even harder to clearly identify the liver [7].

In this paper, we present a Fuzzy C-Means based image segmentation approach, *FCM-Threshold (FCM-t)*. The *FCM-t* uses an optimum threshold, calculated using measure of fuzziness, in order to reveal the ambiguous pixels, which are eventually assigned to the appropriate clusters. The proposed approach will be evaluated on Liver CT images.

The fuzzy approach we follow in this paper is the *information-theoretical approach*, since it is the most used fuzzy tecnhique in literatire due to its simplicity and high speed. This approach,aximizes/minimzes measures of fuzziness and image information such as index of fuzziness or crispness, fuzzy entropy, *etc* [9]. Example of realted work to this approach can be found here [17–21]. The paper is organized as follows: Section 2 gives an overview of the methodology used, describes Fuzzy C-Means Clustering as well as explains how measure of fuzziness is used to find the optimum threshold used for revealing the ambiguous pixels. Section 3 describes the dataset used in this paper. Results are shown in Section 4 and the paper is concluded in Section 5.

2 Methodology

The proposed liver CT image segmentation approach, *FCM-t*, adopted in this paper, is depicted in Fig.1, and described in detail in the following section along with the steps involved and the characteristics feature for each phase and the overall architecture of the introduced approach.

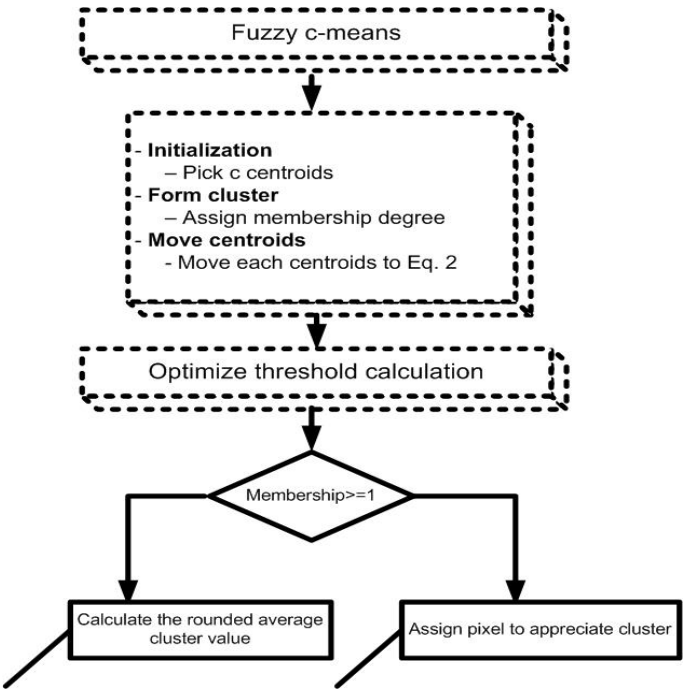

Fig. 1. FCM-t architecture

2.1 Fuzzy C-Means Clustering

Let $X = \{x_1, ..., x_b, ..., x_n\}$ be a set of n objects, and $V = \{v_1, ..., v_b, ..., v_c\}$ be a set of c centroids in a p-dimensional feature space. The Fuzzy C-Means partitions X into c clusters by minimizing the following objective function [8]:

$$J = \sum_{j=1}^{n} \sum_{i=1}^{c} (\mathbf{u}_{ij})^m \left\| \mathbf{x}_j - \mathbf{v}_i \right\|^2 \tag{1}$$

where $1 \leq\ m \leq \infty$ is the *fuzzifier*, $\mathbf{v}_i$ is the i^{th} centroid corresponding to cluster β_i, $\mathbf{u}_{ij} \in [0, 1]$ is the fuzzy membership of the pattern $\mathbf{x}_j$ to cluster β_i, and $\|.\|$ is the distance norm such that,

$$\mathbf{v}_i = \frac{1}{n_i} \sum_{j=1}^{n} (\mathbf{u}_{ij})^m x_j \quad \text{where} \quad n_i = \sum_{j=1}^{n} (\mathbf{u}_{ij})^m \tag{2}$$

and

$$\mathbf{u}_{ij} = \frac{1}{\sum_{k=1}^{c} \left(\frac{d_{ij}}{d_{kj}} \right)^{\frac{2}{m-1}}} \quad \text{where} \quad d_{ij}^2 = \left\| \mathbf{x}_j - \mathbf{v}_i \right\|^2 \tag{3}$$

FCM starts by randomly choosing c objects as centroids (means) of the c clusters. Memberships are calculated based on the relative distance (Euclidean distance) of the object $\mathbf{x}_j$ to the centroids using Eq. (3). After the memberships of all objects have been found, the centroids of the clusters are calculated using Eq. (2). The process stops when the centroids from the previous iteration are identical to those generated in the current iteration [8].

2.2 Measure of Fuzziness

The most common measure of fuzziness is the *linear index of fuzziness.* For an $M \times N$ image subset $A \subseteq X$ with L gray levels $g \in [0, L-1]$, the histogram $h(g)$ and the membership function $\mu_X(g)$, the linear index of fuzziness γl is defined as follows [9]:

$$\gamma l = \frac{2}{MN} \sum_{g=0}^{L-1} h(g) \times min\left[\mu_A(g), 1 - \mu_A(g)\right] \tag{4}$$

The membership function $\mu_X(g)$ used in this paper is Zadeh's *S-Function*, defined as follows [10]:

$$\mu_X(g) = \begin{cases} 0 & \text{if } x \leq a \\ 2\left(\frac{x-a}{c-a}\right)^2 & \text{if } a \leq x \leq b \\ 1 - 2\left(\frac{x-c}{c-a}\right)^2 & \text{if } b \leq x \leq c \end{cases} \tag{5}$$

where $a = 0$, $b = 0.5$, and $c = 1$.

2.3 Optimum Threshold and Ambiguous Pixels

The optimum threshold to be calculated based on measures of fuzziness will be used to reveal the *ambiguous pixels*, such that pixels with membership values greater than or equal to the threshold will be assigned to the appropriate clusters (identified as *1* and *2*), and those pixels with membership values less than the threshold will be marked as ambiguous, and assigned to the appropriate clusters, calculated by rounding to the nearest integer the average of the cluster values in the 3×3 neighbourhood of that uncertain pixel (Fig.3). It should be noticed here that we have calculated an optimum threshold for each cluster.

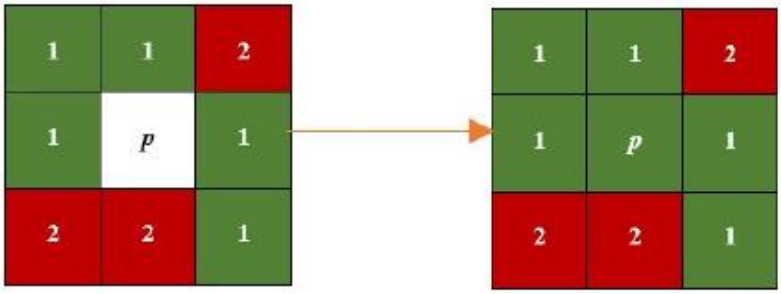

Fig. 2. Assigning the ambiguous pixel to the appropriate cluster

The algorithm for calculating the optimum threshold based on measures of fuzziness is shown in Algorithm (1).

3 Abdominal CT Data Collection

CT scanning is a diagnostic imaging procedure that uses X-rays in order to present cross-sectional images (slices) of the body. The proposed system will be applied on a complex dataset. The dataset is divided into seven categories, depending on the tumor type: Benign (Cyst (CY), Hemangioma (HG), Hepatic

Algorithm 1 Calculating the optimum threshold based on measures of fuzziness algorithm

1: Select the shape of the membership function (*i.e.* S-Function)
2: Select a suitable measure of fuzziness (*i.e.* Eq.(4))
3: Calculate the image histogram
4: Initialize the position of the membership function
5: Shift the membership function along the grey-level range, and calculate in each position the amount of fuzziness, using for instance Eq.(4)
6: Locate the position g_{opt} with maximum fuzziness
7: Threshold the image with $T = g_{opt}$

Adenoma (HA), and Focal Nodular Hyperplasia (FNH)); or Malignant (hepatocellular carcinoma (HCC), Cholangiocarcinoma (CC), and Metastases (MS)). Each of these categories have more than 15-patients, each patient has more than one hundred slices, and more than one phase of CT scan (arterial, delayed, portal venous, non-contrast). The dataset includes a diagnosis report for each patient. All images are in JPEG format, selected from a DICOM file, and have dimensions of 630630, with horizontal and vertical resolution of 72 DPI, and bit depth of 24 bits [12]. All CT images were captured from Radiopaedia[1] .

4 Results and Discussion

The proposed approach, *FCM-t* was tested on 30 Liver CT images. Fig.3 shows examples of applying both the traditional *FCM* and *FCM-t* on those images, provided that 2-clusters were used in each case.

A one-way *MANOVA* analysis was carried out to assess whether both *FCM* and *FCM-T* methods have a statistically significant effect on the segmentation performance. The differences between the two algorithms (*i.e.* independent variable) were analyzed using a one-way *MANOVA* on both *Jaccard Index (JI)* [13,16] and *CPU processing time* (*i.e.* dependent variables). This was considered after checking the assumptions of multivariate normality and homogeneity of variannce/covariance, for a significance of level 5%.

The assumption of normality of each of the univariate dependent variables was examined using a paired-sample *Kolmogorov-Smirnov* (p-*value*<0.05) [14]. Although the univariate normality of each dependent variable has not been verified, since the number of samples is large (n=*30*), this statement can be assumed by considering the *Central Limit Theorem (CLT)* [15]. As such, the assumption of multivariate normality was then validated [15]. Also, note that *MANOVA* makes the assumption that the within-group covariance matrices are equal. Therefore, the assumption about the equality and homogeneity of the covariance matrix in

[1] http://radiopaedia.org/search?q=CTscope=all

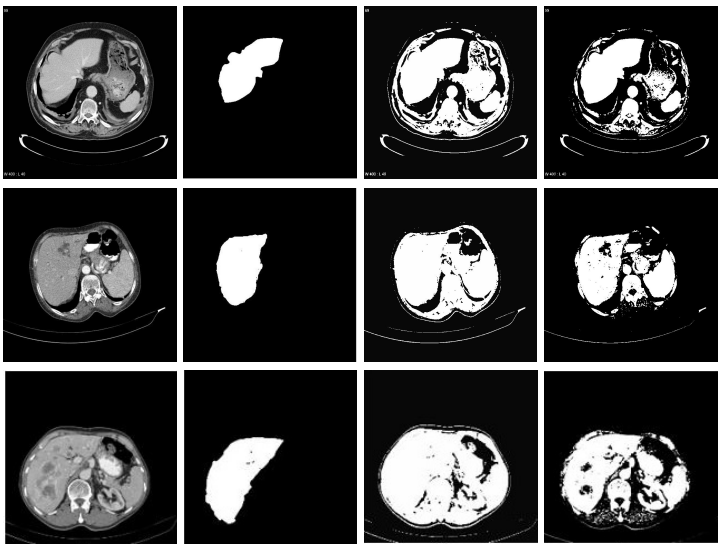

Fig. 3. (a) original image; (b) ground truth of (a); (c) FCM result of (a); (d) FCM-T result of (a); (e) original image; (f) ground truth of (e); (g) FCM result of (e); (h) FCM-T result of (e); (i) original image; (j) ground truth of (i); (k) FCM result of (i); and (l) FCM-T result of (i)

each group was verified with the *Box's M Test* (M=64.6076,F(3;720)=-1.8403; *p-value*=1.0000). This suggests that the design is balanced and, since there is an equal number of observations in each cell (n=30), the robustness of the *MANOVA* tests is guaranteed.

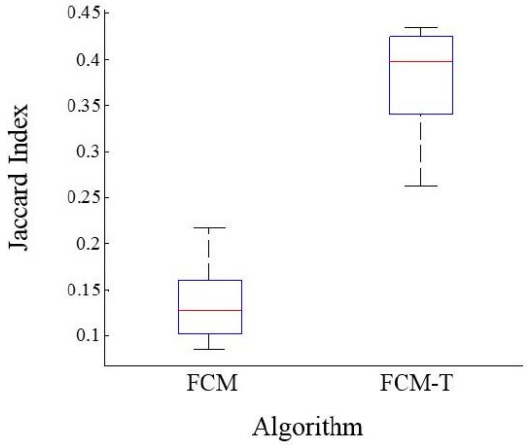

Fig. 4. Box plot of FCM and FCM-t in terms of Jaccard Index

The *MANOVA* analysis revealed that the type of algorithm led to a statistically significant different outcome on the multivariate composite ($F(1; 58)$=130.0100; *p-value*<0.0001). As *MANOVA* detected significant statistical differences, we proceeded to the commonly-used *ANOVA* for each dependent variable. By carrying an individual test on each dependent variable, it was possible to observe that both *JI* ($F(1; 58)$=456.03; *p-value*<0.0001) and *CPU* processing time ($F(1; 58)$=109.33; *p-value*<0.0001) present statistically significant differences between the two methods. The proposed *FCM-t* does present significantly better results than the traditional *FCM*, but at the cost of some processing power. In order to easily assess the differences between both algorithms and further understand the trade-off between performance and algorithmic complexity, let us show the outcome of each trial graphically using box plot charts (refer to Fig.4 and Fig.5). The ends of the blue boxes and the horizontal red line in between correspond to the first and third quartiles and the median values, respectively. As one may observe, by benefiting from the optimum threshold approach, one is able to increase the segmentation performance by approximately three times more than with the traditional *FCM*, while doubling the computational complexity.

5 Conclusion and Future Work

Using an optimum threshold for revealing ambiguous pixels, and then assigning such ambiguous pixels to their appropriate clusters, can provide better segmen-

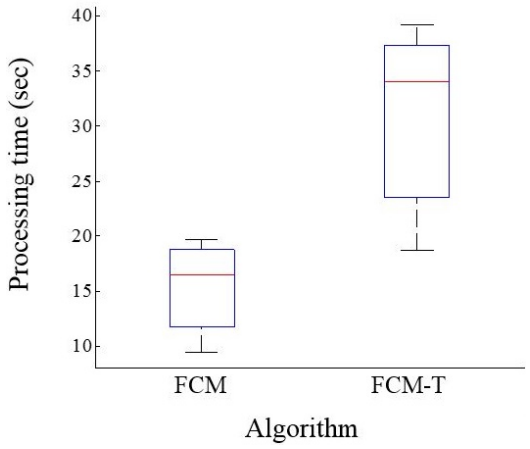

Fig. 5. Box plot of FCM and FCM-t in terms of CPU processing time

tation results. Compared to the traditional Fuzzy C-Means, the proposed approach showed significantly better results in terms of Jaccard Index, although that was at the cost of some processing power. Also, from a visual perspective, the proposed approach in some cases was able to show the ground truth more clearly. As a prospect to this work, we are aiming at providing a post-processing stage were the ground truth will be determined without the surrounding objects, so as to obtain more accurate results. Moreover, we also aim at decreasing the computational complexity of the optimization step by benefiting from stochastic methods, such as the particle swarm optimization algorithm.

Acknowledgment

This work was supported by the Bio-Inspired Methods: research, development and knowledge transfer project, reg. no. CZ.1.07/2.3.00/20.0073 funded by Operational Programme Education for Competitiveness, co-financed by ESF and state budget of the Czech Republic.

References

1. Annadurai, S., Shanmugalakshmi, R.: Fundamentals of Digital Image Processing. Dorling Kindersley, Delhi (2006)
2. Läthén, G.: Segmentation Methods for Digital Image Analysis: Blood Vessels, Multi-scale Filtering, and Level Set Methods. Linköping studies in science and technology, thesis no. 1434 (2010)
3. Huang, X., Tsechpenakis, G.: Medical Image Segmentation. In Information Discovery on Electronic Health Records, V. Hristidis (Editor), Chapman & Hall, Chapter 10 (2009)

4. Leeuwen, M., Noorddzij, J., Feldberg, M., Hennipman, A., Doornewaaard, H.: Focal Liver Lesions: Characterization with Triphasic Spiral CT. Radiology, 201:327-336 (1996)
5. Digestive Disorders Health Center. Retrieved from: http://www.webmd.com/digestive-disorders/picture-of-the-liver. Accessed on 11 March 2014.
6. Bronzino, J.: The Biomedical Engineering Handbook. 2. Springer, Heidelberg (2000)
7. Mharib, A., Ramli, A., Mashohor, S., Mahmood, R.: Survey on Liver CT Image Segmentation Methods. Artificial Intelligence Review, 37(2), 83-95 (2012)
8. Maji, P., Pal, S.: Maximum Class Separability for Rough-Fuzzy C-Means Based Brain MR Image Segmentation. T. Rough Sets, 9, pages 114-134 (2008)
9. Tizhoosh, H.: Image thresholding using type II fuzzy sets. Pattern Recognition. 38(12), 23632372 (2005)
10. Zadeh, L.: Calculus of Fuzzy Restrictions. In L.A. Zadeh, K.S. Fu, K. Tanaka and M. Shimura, eds. Fuzzy Sets and their Applications to Cognitive and Decision Processes, 1-39, Academic Press, New York (1975)
11. Bush, B.: Fuzzy Clustering Techniques: Fuzzy C-Means and Fuzzy Min-Max Clustering Neural Networks. Retrieved from: http://benjaminjamesbush.com/fuzzyclustering/fuzzyclustering.docx. Accessed on 12 March 2014.
12. Anter, A., Azar, A., Hassanien, A., El-Bendary, N., ElSoud, M.: Automatic Computer Aided Segmentation for Liver and Hepatic Lesions Using Hybrid Segmentations Techniques. IEEE Proceedings of Federated Conference on Computer Science and Information Systems 2013, pp.193-198 (2013)
13. Jaccard, P.: Etude Comparative de la Distribution Orale Dansune Portion des Alpes et des Jura. In Bulletin del la Socit Vaudoise des Sciences Naturelles, Vol. 37, pp.547-579 (1901)
14. Peacock, J.: Two-dimensional Goodness-of-fit Testing in Astronomy. Monthly Notices Royal Astronomy Society, vol. 202, pp. 615-627 (1983)
15. Pallant, J.: SPSS Survival Manual, Kindle Edition Ed. Open University Press; 4th edition (2011)
16. Narayana C., Sreenivasa Reddy E., Seetharama Prasad M.: Automatic Image Segmentation using Ultrafuzziness. International Journal of Computer Applications, 49(12):6-13 (2012)
17. Chaira, T., Ray, A.: Segmentation Using Fuzzy Divergence, Pattern Recognition Lett. 24 (12), 18371844 (2003)
18. Huang, L., Wang, M.: Image Thresholding by Minimizing the Measure of Fuzziness, Pattern Recognition 28, 4151 (1995)
19. Pal, N., Bhandari, D., Majumder, D.: Fuzzy Divergence, Probability Measure of Fuzzy Events and Image Thresholding, Pattern Recognition Lett. 13, 857867 (1992)
20. Wang, Q., Chi, Z., Zhao, R.: Image Thresholding by Maximizing the Index of Nonfuzziness of the 2-D Grayscale Histogram, Comput. Vision Image Understanding 85 (2), 100116 (2002)
21. Zenzo, S., Cinque, L., Levialdi, S.: Image Thresholding Using Fuzzy Entropies, SMC 28 (1), 1523 (1998)